Real-World ADS-B signal recognition based on Radio Frequency Fingerprinting

†Haoran Zha, †‡Qiao Tian, †*Yun Lin
†College of Information and Communication Engineering, Harbin Engineering University, Harbin, P.R.China
‡College of Computer Science and Technology, Harbin Engineering University, Harbin, P.R.China
*Corresponding Author: linyun@hrbeu.edu.cn

***Abstract*—To meet the future needs of increasingly crowded airspace, the International Civil Aviation Organization (ICAO) proposed to use the Automatic Dependent Surveillance-Broadcast (ADS-B) to provide navigation and surveillance technology to solve the problems of security and capacity in the airspace. But ADS-B does not offer any authentication and encryption. So it is vulnerable to attacks by various illegal devices. A novel radiofrequency fingerprint (RFF) recognition method of aircraft identity verification based on deep learning is proposed. The ADS-B signal captured by RTL-SDR is used for confirmation. The experimental results show that the fingerprint is called the Contour Stellar Images with a better recognition effect under different networks and different SNR.**

***Index Terms*—Radio Frequency Fingerprinting, ADS-B, Signal Detection, Deep Learning**

I. Introduction

By 2030, the Air Traffic Control (ATC) technology currently in use will quickly reach its capacity limit [1]. To replace traditional primary and secondary surveillance radar methods, the International Civil Aviation Organization has adopted a new protocol standard called Automatic Dependent Surveillance-Broadcast (ADS-B) [2]. ADS-B is to collect navigation information by the airborne information processing unit, and then broadcast it through the airborne communication equipment. There is no need for both parties to agree on other communication protocols [3]. Compared with radar, ADS-B has a shorter construction period, a smaller investment, and more accurate and real-time monitoring information, which can fill the blind area of radar free area and reduce the demand and dependence of existing radar area on radar [4]. For the aircraft equipped with ADS-B receiver, combining all the broadcast information and the received monitoring information with its location information, it can form a more intuitive and three-dimensional surrounding traffic information for the pilot. ADS-B combines navigation and monitoring information in the same system. Any aircraft equipped with ADS-B system broadcasts the location information through the public communication channel, so that any aircraft equipped with ADS-B receiver can get a complete monitoring image by combining the heard broadcast, received monitoring information and its position, which dramatically improves the monitoring efficiency. It can be predicted that the ADS-B system, combined with a wide-area multi-point positioning system and S-mode radar, will gradually eliminate the current secondary surveillance sensor, which is an integral part of the new navigation system. Nevertheless, the ADS-B protocol was proposed about 20 years ago, and the ADS-B protocol does not provide any encryption and authentication methods. Due to the advent of cheap and accessible software-defined radios, today, anonymous devices can be attacked using widely available SDRs [5].

978-1-7281-6992-7/20/$31.00 ©2020 IEEE

Deep learning (DL) is a new research field in machine learning, which benefits from the improvement of big data and hardware [6]. DL has recently gained attention because of the successful applications in computer vision (CV) [7], natural language processing (NLP) [8]Researchers are interested in trying to extend DL to other domains, including Individual identification [9]. Compared to traditional Machine Learning (ML), DL can perform further performance improvements, since DL have a flexible mechanism to extract feature itself to optimize the parameter to get a better end to end performance. Though DL has many merits [10], its downsides should not be ignored. Due to the lack of vital data support, the DL pattern is likely to overfit for its deep and complex structure. Convolutional Neural Networks (CNN) [11] is the main framework of DL in the CV. There have been several works studying on the application of DL in Automated Modulation Classification (AMC) [12], paper state by using Spectral Correlation Function (SCF) pattern, and Deep Belief Network (DBN) to develop AMC [13]. This paper solves the AMC problem in Cr by classifying involved CNN. To fully exploit the potential of CNN, Yao YuDong, and his students perform the famous CNN model [14], AlexNet, and GoogleNet, and use three-channel images for modulation recognition, it does get excellent efficiency.

Equipment identification based on radio frequency fingerprint (RFF) [15] is a new physical layer (PHY) security technology, which is used to distinguish the identification of wireless devices. It can be used in many Internet of things (IoT) purposes, such as vehicle communication [16], electronic license plate authentication [17], and can be used for aircraft classification and detection. There are subtle differences between wireless elements due to fabrication defects. These differences, known as RFF, are unique and persistent and can be seen as the ”DNA” of the construction [18]. RFF will be presented in the signal waveform. RFF identification designs advanced signal processing protocol to

https://t.me/learningnets

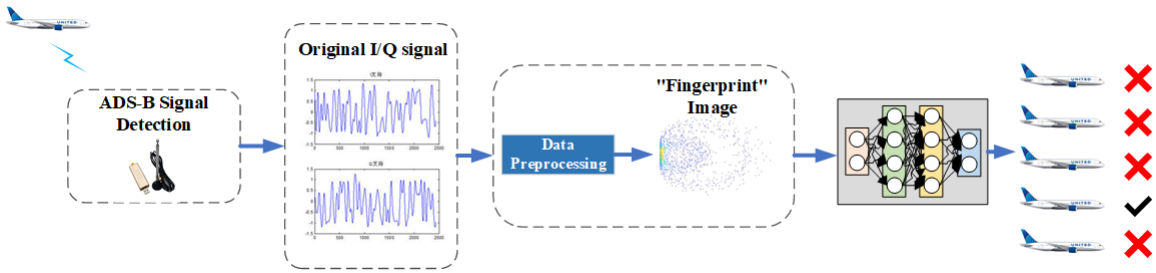

Fig. 1. Aircraft fingerprint recognition.

extract these unique and inherent physical features of each device to establish user identity [19].

RFF recognition usually consists of training and classification, which is a classical drudge learning classification problem. However, to get stable I / Q samples for training and verification, it is necessary to have prior knowledge of carrier frequency and time synchronization. Besides, due to the complexity, the length of the I / Q sequence in the existing sample-based CNN scheme is usually concise, which leads to inadequate recognition accuracy [20]. Due to the successful promotion of CNN in image recognition, the complex classification task has been developed. In this paper, we use CNN to classify Contour Stellar Images obtained by different devices. Unlike most of the RFF recognition schemes using sample-based CNN, this scheme uses a pattern similar to fingerprint to classify different targets, which is called image-based CNN directly. Fig. 1 shows the process of Aircraft fingerprint recognition.

The main contributions of this article are as follows:

1. We propose and design a novel RFF recognition scheme based on the Contour Stellar Images and CNN. The generated equipotential planet map is similar to the ”fingerprint” graphic, so it can be identified using image recognition CNN.

2. We proposed an ADS-B original signal detection acquisition and real-time labeling method and verified this method by using a 1090MHz baseband signal collected by RTL-SDR, collecting signals from a total of 5 aircraft, 500 signals were selected uniformly for each aircraft.

3. We compared the performance of Contour Stellar images and Constellation Diagram under the Alexnet network and different signal-to-noise ratioSNR. Besides, we also compared the performance of Contour Stellar images on Alexnet and GoogleNet.

The rest of this paper is organized as follows. In Section II, we introduce ADS-B signals and the datasets used in the rest of the paper. In Section III, we present signal preprocessing. In Section IV, we discuss the experimental results, and finally, in Section V we summarize the paper.

An aircraft reclaims its position and velocity using an onboard spy-in-the-sky receiver. This information is sent twice per second by the transmitting subsystem ADS-B Out. They are sustained by ground stations and by nearby aircraft if equipped with ADS-B In, where they are concocted further (e.g., by collision avoidance systems such as TCAS). ADS-B offers many further fields such as ID, intent, urgency code, and navigation accuracy/uncertainty level. Two ADS-B data link standards are currently in use, Universal Access Transceiver(UAT) and 1090 MHz Extended Squitter(1090ES) [2].

1090 MHz Extended Squitter(1090ES) is a technology-based on S-mode transponder, with a frequency of 1090MHz. The format of the ADS-B message data block utilizes Pulse Position Modulation (PPM) coding. The first half of each transmitted pulse is 1, and the second half is 0. A complete ADS-B signal is composed of 8us preamble pulse and 112us data information bit pulse [3], as shown in Fig. 2.

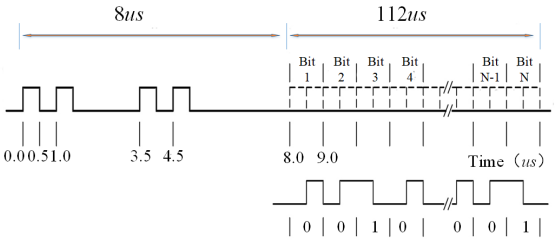

Fig. 2. ADS-B signal structure [21].

We use the relatively low-cost software radio RTL-SDR as the signal source. The RTL-SDR communicates with the PC through the USB interface, the RTL-SDR Architecture and workflow are shown in Fig. 3.

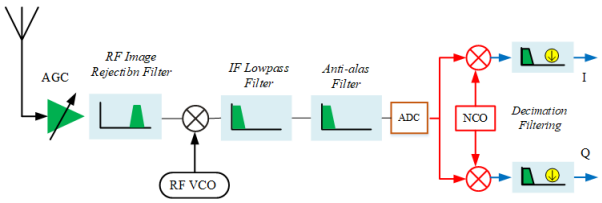

Fig. 3. RTL-SDR Architecture and workflow.

After receiving the RF signal containing ADS-B signal from the antenna, the received signal shall first be amplified by automatic gain control (AGC), and then throughRF Image Rejectibn Filter filter. Image Rejectibn Filter is a band-pass filter, which filters out unnecessary image signal, and then

https://t.me/learningnets

mixes the signal. Set RF signal freqyenc as f_c, intermediate frequence as f_{if}, and initial ADS-B signal as:

$$e_{adsb}(t) = s(t)\cos\left(2\pi f_c t + \varphi_0\right) \tag{1}$$

In this formula

$$s(t) = \sum_m a_m g\left(t - mT_a\right) \tag{2}$$

Where a_m is the baseband symbol, T_a is the chip duration, $g(t)$ is a rectangular pulse of a certain width, then the frequency of the sine wave generated by VCO is $f_{lo} = f_c - f_{ij}$, the RF signal and the sine wave generated by VCO are mixed:

$$\begin{aligned} e_{adsbmix}(t) =& s(t)\cos\left(2\pi f_c t + \varphi_0\right)\cos\left(2\pi f_{lo} t\right) \\ =& \frac{s(t)}{2}\cos\left[\left(2\pi\left(f_c + f_{lo}\right)t + \varphi_0\right)\right. \\ &+ \cos\left[\left(2\pi\left(f_c - f_{lo}\right)t + \varphi_0\right)\right] \end{aligned} \tag{3}$$

The high frequency component is attenuated by the IF low-pass filter, and only the IF component is transmitted forward to the next level:

$$e_{adsbif}(t) = \frac{s(t)}{2}\cos\left(2\pi f_{if} t + \varphi_0\right) \tag{4}$$

We sample $e_{adsbif}(t)$ in formula (4) with $T_s = 1/f_{adc}$ and get the following data:

$$e_{adsbif}(n) = \sum_m a_m g\left(nT_s - mT_a\right)\cos\left(\omega_c n + \varphi_0\right) \tag{5}$$

In formula (5) , $\omega_c = 2\pi f_{if}/f_{\text{adc}}$, Obtain IQ signal through NCO and low-pass filtered:

$$\begin{aligned} z_{BI}(n) &= \textstyle\sum_m a_m g\left(nT_s - mT_a\right)\cos\left(\varphi_0\right) \\ z_{BQ}(n) &= \textstyle\sum_m a_m g\left(nT_s - mT_a\right)\sin\left(\varphi_0\right) \end{aligned} \tag{6}$$

Then the IQ signal is decoded by using the relevant decoding algorithm , the total data collection and labeling process is shown in Fig. 4.

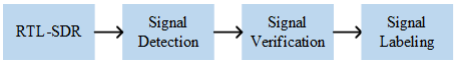

Fig. 4. The total ADS-B signal collection and labeling process.

The reception, detection, annotation, training and classification of ADS-B signals are implemented on the system shown in Fig. 5.

We collected data from a total of 5 aircraft at fixed locations. Each aircraft randomly selected 500 original baseband IQ signals, and each signal was annotated with an ICAO code. And then, we divided the data into training and validation data sets. We use 70% of the signal for training and 30% for validation. Avoid class imbalance in ADS-B data by ensuring a uniform distribution of labels (Aircraft types). Fig. 6 show the label distributions to check if the generated labels are uniformly distributed.

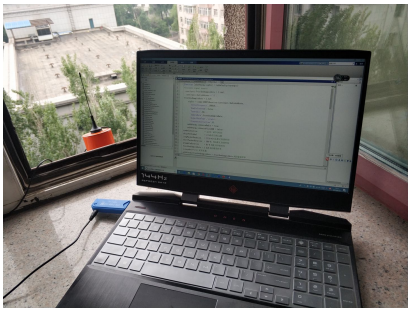

Fig. 5. Implemented on the system.

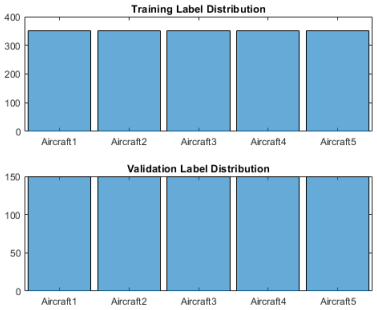

Fig. 6. Label distributions.

II. Signal Preprocessing

In RFF classification, the data to be concocted is not an image, but complex IQ data samples are shown in formula (6). To manipulate the existing DL models, we transform complex data samples into the Contour Stellar images for DL. The first step in data processing is to plot the signal into the form of a Constellation diagram. And then, we color the Constellation diagram according to the normalized dot density of each point in the Constellation picture [22]. Furthermore, the normalized point density of the $p-th$ symbol in each sample, $\rho(p)$ is calculated as follows:

$$\rho(p) = \frac{\sum_{j=1}^{N} g[h(p) - h(j)| < r \&\& |v(p) - v(j)| < r]}{N} \tag{7}$$

Where $h(p)$ function and $v(p)$ function obtain the horizontal axis and the vertical axis value of the $p-th$ symbol, N is the number of the symbols of this sample, r is half the length of the selected rectangular region when determining the normalized point density. The product of $g(\bullet)$ satisfies the following formula:

$$f(x) = \begin{cases} 1, & x = \text{ True} \\ 0, & x = \text{ False} \end{cases} \tag{8}$$

Then, every point in the Constellation diagram will be colored according to the color bar shown in Fig. 7. and its normalized point density. The overall calculation formula of the contour stellar images is as follows:

https://t.me/learningnets

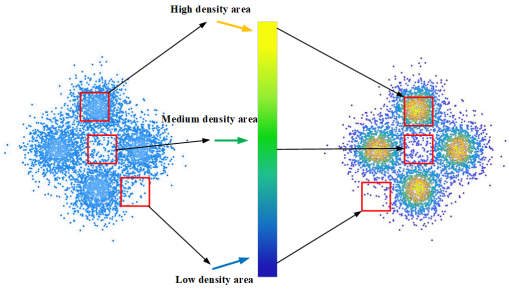

Fig. 7. Constellation Diagram Converted To Contour Stellar Images.

$$\rho(p,j) = \frac{\sum_{p=x_1}^{x_2} \sum_{j=y_1}^{y_2} \mathrm{dots}(p,j)}{\sum_{x_1=W_0}^{W_1} \sum_{y_1=H_0}^{H_1} \sum_{p=x_1}^{x_2} \sum_{j=y_1}^{y_2} \mathrm{dot}\, S(p,j)} \tag{9}$$

Where W_0 , H_0 are the upper left corner coordinates of the contour stellar images, W_1 , H_1 are lower right corner coordinates the contour stellar images, x_0 , y_0 are the upper left coordinate of the density window function, x_1 , y_1 are the lower right corner of the density window function. Fig. 8 shows the contour stellar images of the 5 aircraft ADS-B signals we captured;

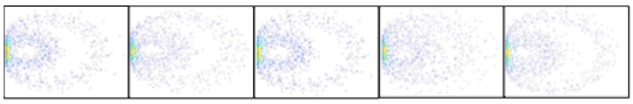

Fig. 8. The Contour Stellar Images of 5 aircraft ADS-B signals.

III. Experiments and Discussion

We use two well known trained CNNs, GoogLeNet(Szegedy et al.2014) [12] and AlexNet (Krizhevsky, Sutskever, and Hinton 2012) [23]. Both networks have engaged in ImageNet Contest in different years with excellent results. The networks differ in general architecture. GoogLeNet has Inception Modules, which perform different sizes of convolutions and concatenate the filters for the next layer. AlexNet, on the other hand, has layers input presented by one previous layer instead of a filter connection. Both networks have been tested independently and use the implementation provided by Matlab Deep Learning Toolbox.

The first part of the Layers section of the network is the image input layer. For a GoogLeNet network, this layer needs input images of size 224-by-224-by-3 [24], where 3 is the number of color channels, the AlexNet network requires images of size 227-by-227-by-3 [12]. Nevertheless, the images ADS-B signal transformed have different sizes. We use a marketed image datastore to resize the training pictures. Define additional augmentation procedures to work on the training images: randomly flip the training images along the vertical axis and randomly turn them up to 30 pixels and balance them up to 10 horizontally and vertically. Data augmentation attends to prevent the network from overfitting and to memorize the training images' exact details.

The convolutional layers of the network extract image feature that the last learnable and final classification layers use to classify the input image. These two layers, 'loss3-classifier' and 'output' in GoogLeNet, comprise how to combine the features that the network extracts into class probabilities, a loss value, and predicted labels. To retrain a pre-trained network to classify new images, We succeed in these two layers with new layers adjusted to the ADS-B dataset.

In AlexNet and GoogLeNet networks, the last layer with learnable weights is fully connected. Replace this fully connected layer with a new fully-connected layer with the number of outputs equal to the number of classes in the ADS-B dataset. We classify the validation images using the fine-tuned network and calculate the classification precision. The test precision of ADS-B data in AlexNet and GoogLeNet networks is 98.66% and 97.87%, Fig. 9 and Fig. 10 show the networks' Confusion Matrix.

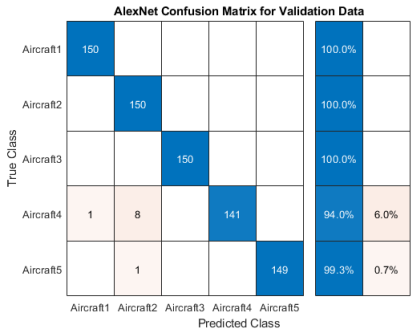

Fig. 9. AlexNet Confusion Matrix for Validation Data.

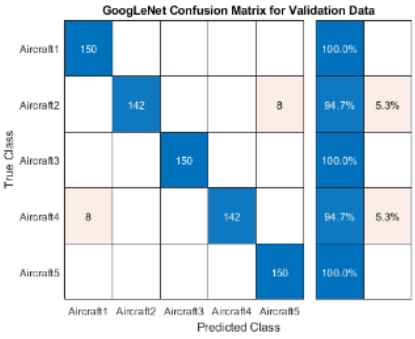

Fig. 10. GoogLeNet Confusion Matrix for Validation Data.

To cover the classification performance at different noise levels, we added additive white Gaussian noise to the test data for experiments. Fig. 10.show the classification performance of Contour Stellar Images at different noise levels. It should be noted that the signal-to-noise ratio(SNR) here refers to the SNR after noise is enumerated when we regard the original signal as a pure signal without noise(in fact, the original signal itself also contains noise). Therefore, the

https://t.me/learningnets

actual SNRs are more diminutive than those shown in the figures. It can be seen that although these noisy samples have not been trained, the Contour Stellar Images have the excellent performance to classify these noisy samples. When the SNR is greater than 28 dB, the classification accuracy under both datasets is higher than 95%. Also, comparing the classification accuracy of Alexnet and GoogLenet at different SNRs, the Alexnet classification is more robust to noise.

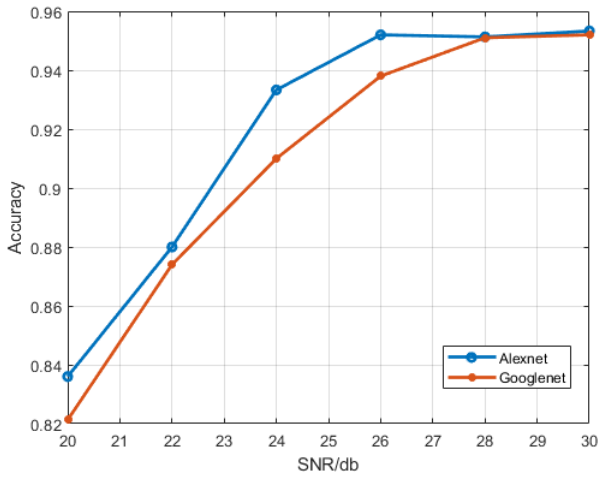

Fig. 11. Classification performance of Contour Stellar Images at different noise levels.

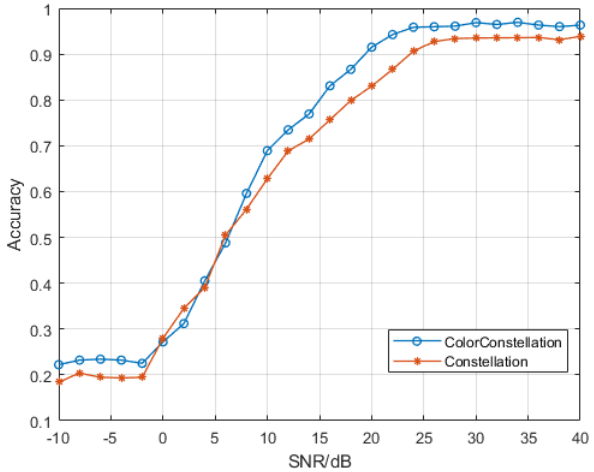

Fig. 12. Classification performance of Contour Stellar Images and Constellation Diagram at different noise levels.

IV. Conclusion

We propose and design a novel RFF recognition scheme based on Contour Stellar Images and deep learning. We designed an ADS-B original signal capture and labeling method and verified this method by using a 1090MHz baseband signal collected by RTL-SDR, collecting signals from a total of 5 aircraft, 500 signals were selected uniformly for each aircraft. Besides, the experimental conclusions under different signal-to-noise ratios and different networks show the effectiveness of the Contour Stellar Images, and it shows that the excellent identification performance of the RF fingerprint can lay a foundation for the physical layer security of aircraft.

Acknowledgment

This work was supported by Scientific Research Foundation for Teachers (No.3072020CFJ0603). The authors would like to thank all coauthors of this work.

References

[1] Li T, Wang B. Sequential collaborative detection strategy on ADS-B data attack[J]. International Journal of Critical Infrastructure Protection, 2019, 24: 78-99.

[2] Schfer M, Strohmeier M, Lenders V, et al. Bringing up OpenSky: A large-scale ADS-B sensor network for research[C]//IPSN-14 Proceedings of the 13th International Symposium on Information Processing in Sensor Networks. IEEE, 2014: 83-94.

[3] Strohmeier M, Schfer M, Lenders V, et al. Realities and challenges of nextgen air traffic management: the case of ADS-B[J]. IEEE Communications Magazine, 2014, 52(5): 111-118.

[4] Thumbur G, Gayathri N B, Reddy P V, et al. Efficient pairing-free identity-based ADS-B authentication scheme with batch verification[J]. IEEE Transactions on Aerospace and Electronic Systems, 2019, 55(5): 2473-2486.

[5] Ying X, Mazer J, Bernieri G, et al. Detecting ADS-B Spoofing Attacks using Deep Neural Networks[C]//2019 IEEE Conference on Communications and Network Security (CNS). IEEE, 2019: 187-195.

[6] Du L, Du Y, Li Y, et al. A reconfigurable streaming deep convolutional neural network accelerator for Internet of Things[J]. IEEE Transactions on Circuits and Systems I: Regular Papers, 2017, 65(1): 198-208.

[7] Gopalakrishnan K, Khaitan S K, Choudhary A, et al. Deep convolutional neural networks with transfer learning for computer vision-based data-driven pavement distress detection[J]. Construction and Building Materials, 2017, 157: 322-330.

[8] Young T, Hazarika D, Poria S, et al. Recent trends in deep learning based natural language processing[J]. ieee Computational intelligenCe magazine, 2018, 13(3): 55-75.

[9] Ziatdinov M, Dyck O, Maksov A, et al. Deep learning of atomically resolved scanning transmission electron microscopy images: chemical identification and tracking local transformations[J]. ACS nano, 2017, 11(12): 12742-12752.

[10] Ghasemi F, Mehridehnavi A, Perez-Garrido A, et al. Neural network and deep-learning algorithms used in QSAR studies: merits and drawbacks[J]. Drug Discov. Today, 2018, 23(10): 1784-1790

[11] Shin H C, Roth H R, Gao M, et al. Deep convolutional neural networks for computer-aided detection: CNN architectures, dataset characteristics and transfer learning[J]. IEEE transactions on medical imaging, 2016, 35(5): 1285-1298.

[12] OShea T J, Corgan J, Clancy T C. Convolutional radio modulation recognition networks[C]//International conference on engineering applications of neural networks. Springer, Cham, 2016: 213-226.

[13] Mendis G J, Wei J, Madanayake A. Deep learning-based automated modulation classification for cognitive radio[C]//2016 IEEE International Conference on Communication Systems (ICCS). IEEE, 2016: 1-6.

[14] Peng S, Jiang H, Wang H, et al. Modulation classification based on signal constellation diagrams and deep learning[J]. IEEE transactions on neural networks and learning systems, 2018, 30(3): 718-727.

[15] Satija U, Trivedi N, Biswal G, et al. Specific emitter identification based on variational mode decomposition and spectral features in single hop and relaying scenarios[J]. IEEE Transactions on Information Forensics and Security, 2018, 14(3): 581-591.

[16] Steinmetz E, Wildemeersch M, Quek T Q S, et al. Packet reception probabilities in vehicular communications close to intersections[J]. IEEE Transactions on Intelligent Transportation Systems, 2020.

https://t.me/learningnets

[17] Saadouli G, Elburdani M I, Al-Qatouni R M, et al. Automatic and Secure Electronic Gate System Using Fusion of License Plate, Car Make Recognition and Face Detection[C]//2020 IEEE International Conference on Informatics, IoT, and Enabling Technologies (ICIoT). IEEE, 2020: 79-84.
[18] Chen Y, Wen H, Song H, et al. Lightweight one-time password authentication scheme based on radio-frequency fingerprinting[J]. IET Communications, 2018, 12(12): 1477-1484.
[19] Peng L, Zhang J, Liu M, et al. Deep learning based RF fingerprint identification using differential constellation trace figure[J]. IEEE Transactions on Vehicular Technology, 2019, 69(1): 1091-1095.
[20] Dai Z, Li L, Xu W. Cfo: Conditional focused neural question answering with large-scale knowledge bases[J]. arXiv preprint arXiv:1606.01994, 2016.
[21] Amrhar A, Kisomi A A, Zhang E, et al. Multi-Mode reconfigurable Software Defined Radio architecture for avionic radios[C]//2017 Integrated Communications, Navigation and Surveillance Conference (ICNS). IEEE, 2017: 2D1-1-2D1-10.
[22] West N E, O'Shea T. Deep architectures for modulation recognition[C]//2017 IEEE International Symposium on Dynamic Spectrum Access Networks (DySPAN). IEEE, 2017: 1-6.
[23] Su L, Ma L, Qin N, et al. Fault diagnosis of high-speed train Bogie by residual-squeeze net[J]. IEEE Transactions on Industrial Informatics, 2019, 15(7): 3856-3863.
[24] Zhang X, Zhou X, Lin M, et al. Shufflenet: An extremely efficient convolutional neural network for mobile devices[C]//Proceedings of the IEEE conference on computer vision and pattern recognition. 2018: 6848-6856.

https://t.me/learningnets